*Original scientific paper*

# Electrochemical treatment of trypan blue synthetic wastewater and its degradation pathway

ANANTHA N. SUBBA RAO and VENKATESHA T. VENKATARANGAIAH⊠

*Department of P.G. Studies and Research in Chemistry, School of Chemical Sciences, Kuvempu University, Shankaraghatta-577451, Shimoga, Karnataka, India*

⊠Corresponding Authors: E-mail: drtvvenkatesha@yahoo.co.uk, Tel.: +91-9448855079; fax: +91-08282-256255.

---

### Abstract

*The trypan blue (TB) dye synthetic wastewater was treated in presence of chloride ions by electrochemical method. The effect of current density, pH, initial concentration of dye and supporting electrolyte on color and COD removal were investigated. The UV-Vis absorption intensity, chemical oxygen demand (COD), cyclic voltammetry (CV), Fourier transform-infrared spectroscopy (FT-IR), gas chromatography – mass spectrometry (GC-MS) analysis were conducted to investigate the kinetics and degradation pathway of TB dye.*

### Keywords

Cataract, Teratogenic, Carcinogenic, Niagara blue, Diamine blue, Decolorization, COD removal, Active anode, Oxidants, Indirect oxidation.

---

## Introduction

Dyes find extensive applications in industries like textile, leather, pulp and paper, printing, photographs [1]. The wastewater from these industries is therefore loaded with the dyes. It is aesthetically unbearable and can turn out to be fatal if this wastewater is allowed to combine with the natural water resources. The presence of dyes or organic molecules increases the biological oxygen demand (BOD), chemical oxygen demand (COD) and total organic carbon (TOC) content of natural water, which especially poses challenges to the survival of aquatic life besides causing serious health hazards leading to the imbalance in ecology [2-4].
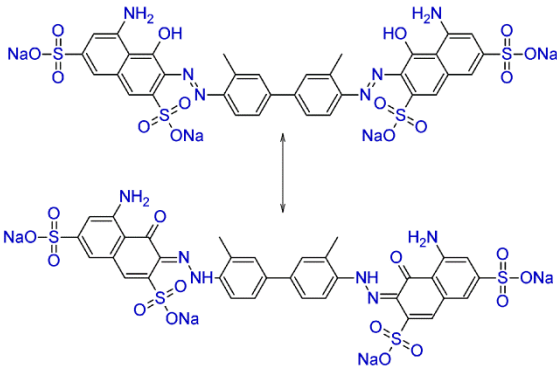
Chemical, physical, biological, and advanced oxidation processes are in practice to treat the wastewater. The electrochemical method is efficient, less time consuming and it does not require the addition of any chemical reagent. In this method, the organic pollutant is oxidized either by

direct electron exchange with the anode (direct oxidation) or by the electrochemically generated oxidants (indirect oxidation). Direct oxidation is possible if the organic pollutant is oxidizable within the overpotential of oxygen (OER) and hydrogen evolution reactions. Indirect oxidation is brought about by the oxidants generated during electrolysis, such as hydroxyl radical ($^•$OH). Hydroxyl radical ($^•$OH, $H^+/H_2O$) is a powerful oxidizing agent with standard reduction potential of 2.7 V *vs.* standard hydrogen electrode. Active chlorine species (oxidants) like $Cl_2$, $Cl_3^-$, $ClO_2^-$, $ClO_3^-$, HOCl, $ClO^-$ are generated in presence of chloride electrolyte and these species can oxidize the organics into simple biodegradable molecules [5,6].

The electrochemical degradation of methyl violet 2B, acridine, eosin yellow [7], alphazurine dye [8], reactive blue 81, reactive red 2 [9], reactive blue-4, reactive orange-16 [10], reactive red 120 [11], reactive brilliant red K-2BP [12], methyl green [13], methyl red [14] and other dyes has been successfully achieved in presence of suitable electrolyte and operating conditions. Furthermore, the results from these works infer that the extent of degradation of an organic pollutant not only depends on the operating conditions employed, but also on the structural, chemical and electrochemical properties of the pollutant itself [7]. The nature of the electrolyte and its concentration, electrode material, pH, current density, wastewater flow rate (stirring rate) and the mechanism of oxidation also significantly influence the extent of degradation of organics. Complete incineration of organics with high efficiency can be achieved by electrochemical method under optimum conditions.

The molecules *o*-tolidine, benzidine and *o*-dianisidine are carcinogenic in nature [16,17]. Trypan blue (TB) (Congo blue 3B / Niagara blue 3B / Diamine blue 14) is an o-tolidine based diazo dye, well known for its ability to selectively color the dead cells blue. It is also used in the dyeing of textiles, leather and paper [18].

*Table 1: Properties and structure of Trapan blue*

| Properties | Chemical structure |
| --- | --- |
| Molecular formula: $C_{34}H_{24}N_6Na_4O_{14}S_4$ <br><br> Molecular weight: 960.8 <br><br> Color Index number: 23850 <br><br> $\lambda_{max}$ / nm = 590 [19] |  |

TB dye (Table I) emerged as one of the most frequently used staining agent in cataract, as well as other anterior segment surgeries in the late 1990s [20]. However, there are reports which unveil the complications in cataract surgery with the usage of TB. C Lüke *et al.* [21] reported the toxic effects of TB after a short duration of retinal exposure and recommended minimizing the usage of TB in intraocular applications [20,22]. TB carries associated risk at higher concentrations and longer duration of exposure [20-22]. Long term presence of 0.2 % TB can cause considerable damage to the retina [23]. International Agency for Research on Cancer provides sufficient eviden-ces for the carcinogenic and teratogenic effects of TB in animals and possibly in humans [24,25].

The photocatalytic degradation of TB is reported in the literature [15,26] but there are no work solely focused on the degradation of TB by electrochemical method [15]. In the present work, the electrochemical oxidation of TB with Pt as anode material has been investigated and probable degradation pathway of TB has been proposed.

**Materials and Chemicals**

*Chemicals*

Commercially available trypan blue (TB) dye was (purchased from HiMedia, Mumbai, India) used for the studies. Analytical grade NaCl, $Na_2SO_4$, $Na_2CO_3$ and $NaNO_3$ and their aqueous solutions were (HiMedia Laboratories Pvt. Ltd, Bangalore, India) used as electrolytes. pH of each electrolyte was adjusted by $H_2SO_4$ and NaOH. The dil. $HNO_3$ was used for the pretreatment of electrodes (HiMedia Laboratories Pvt. Ltd, Bangalore, India).

*Experimental*

A single compartment glass container was used as electrolytic cell (6.5 cm diameter x 10 cm height, covered with Teflon® lid provided with gaps to insert the electrodes). Two Pt foils (dimension 0.5 cm × 0.5 cm, thickness 0.018 cm, supplied by Systronics India Ltd. Bangalore, India) of surface area, 0.54 $cm^2$ were used as anode and cathode which were separated by 0.5 cm in the electrolytic cell. The potentials of working electrode (anode) were recorded relative to saturated calomel electrode (SCE). A DC source with galvanostatic mode (Model PS-618 chemilink systems, Navi Mumbai, India) was used for power supply. The synthetic wastewater of TB dye was prepared with ultrapure water obtained from Elix 3 Milli-pore system (resistivity, > 18 MΩ cm at 25 °C). A magnetic stirrer (550 rotations per minute) was used for the agitation of wastewater during electrolysis.

*Electrolysis*

The solution with the composition of 50 mg $L^{-1}$ TB dye solution and NaCl, 0.2 % was prepared in Millipore water and was subjected to electrolysis under galvanostatic condition for 60 minutes. The Pt electrodes were dipped in dilute $HNO_3$, sonicated for 1 minute and thoroughly washed with Millipore water. All experiments were carried out at ambient temperature. To monitor the progress of the degradation process, electrolyzed samples were collected at appropriate time intervals and subjected to analysis. The effect of current density, pH, nature of electrolyte and its concentration on COD and color removal efficiency was examined. The optimum condition for the maximum color and COD removal efficiency was determined.

*Analysis*

Cyclic voltammetry (CV)

The cyclic voltammetric measurements were performed at room temperature with conventional three electrode system connected to software controlled electrochemical work station (CH Instruments 660C, USA). The working electrode was a Pt disk and counter electrode was a Pt foil. The working electrode surface was polished with 0.05 μm alumina, washed with methanol, dipped in 10 % $HNO_3$, sonicated for 2 min and then washed thoroughly with Millipore water before use. The open circuit potential was recorded in 0.2 % NaCl solution and the potential window from +1.1 V to -1.1 V was selected for CV scans. CV for blank solution (0.2 % NaCl) and TB dye solution (50 mg $L^{-1}$ + NaCl 0.2 %) were recorded at the scan rate of 100 mV $s^{-1}$.

Spectroscopic and chemical analysis

The extent of degradation was monitored by evaluating color and COD removal. UV-Vis absorbance spectra of samples were recorded by Ocean Optics UV-Vis HR 4000 spectro-photometer (UV-Vis-NIR light source, DT-MINI-2-GS and Jaz detector). The percentage color removal was calculated by using the relation (1) with reference to the absorption intensity at $\lambda_{max}$ of 590 nm.

$$\text{Color removal}, \% = \frac{[Abs_0 - Abs_t]}{Abs_0} \times 100 \tag{1}$$

Where $Abs_0$ and $Abs_t$ are the absorbance at 590 nm at time 0 and $t$ minutes of electrolysis respectively.

The COD $(g(O_2)\,L^{-1})$ estimation was carried out by open reflux method and its values used to monitor the progress in degradation. The percentage COD removal was calculated using the relation (2).

$$\text{COD removal}, \% = \frac{[COD_0 - COD_t]}{COD_0} \times 100 \tag{2}$$

Where $COD_0$ and $COD_t$ are the COD at time 0 and $t$ minutes of electrolysis respectively.

The percentage average current efficiency (ACE) was calculated using the following relation (3) [6].

$$\text{ACE}, \% = \frac{[COD_0 - COD_t]FV}{8It} \times 100 \tag{3}$$

Where $F$ is the Faraday's constant (96,485 C mol$^{-1}$), COD in (g O$_2$ L$^{-1}$), $I$ is the current (A), $V$ is the volume (L) of electrolyte, $t$ – time (s), 8 – gram equivalent mass of oxygen (g equiv$^{-1}$).

To determine the degradation pathway, the test samples at selected time intervals (15 and 40 min) were subjected to freeze drying using Lyophilizer (Delvac, India) at -50 ± 5 °C under reduced pressure of 0.12 mbar. Freeze drying eliminates the chances of decomposition of intermediates and only the volatile compounds are removed. The solid residue thus obtained was subjected to UV-Vis spectroscopy, Fourier Transform Infrared Spectroscopy FT-IR (Alpha, Brucker) and gas chromatography mass spectrometry (GC-MS) analyses. The solid residue was finely mixed with KBr, pressed into a disk and subjected to FT-IR analysis. The FT-IR spectrums recorded are the average 16 scans from wave number 4000 cm$^{-1}$ to 500 cm$^{-1}$. GC-MS analysis was carried out in order to detect the end products of TB degradation. The samples were analyzed using GC-MS system (Trace GC Ultra and Trace DSQ THERMO-Electron Corporation, Austin, TX, USA) with a HP-5MS, 5 % phenyl methyl silox column (30 m × 0.25 mm, film thickness 0.25 μm). A temperature gradient program at 10° C min$^{-1}$ was applied between 40 °C and 250 °C.

## Results and Discussion

### Cyclic Voltammetry Studies

The cyclic voltammograms are shown in Fig. 1. A peak at -0.23 V was observed during cathodic sweep of blank solution. The hydrogen evolution begins approximately at -0.80 V. The voltammogram obtained for the dye solution showed the same pattern as the blank and no new peak was observed during the anodic sweep. This indicates that the TB dye does not undergo direct electrochemical reaction on Pt in the potential range from -1.1 to +1.1 V. The decrease in anodic peak (at -0.80 V *vs.* SCE) current can be attributed to the adsorption of dye on the surface of working electrode.
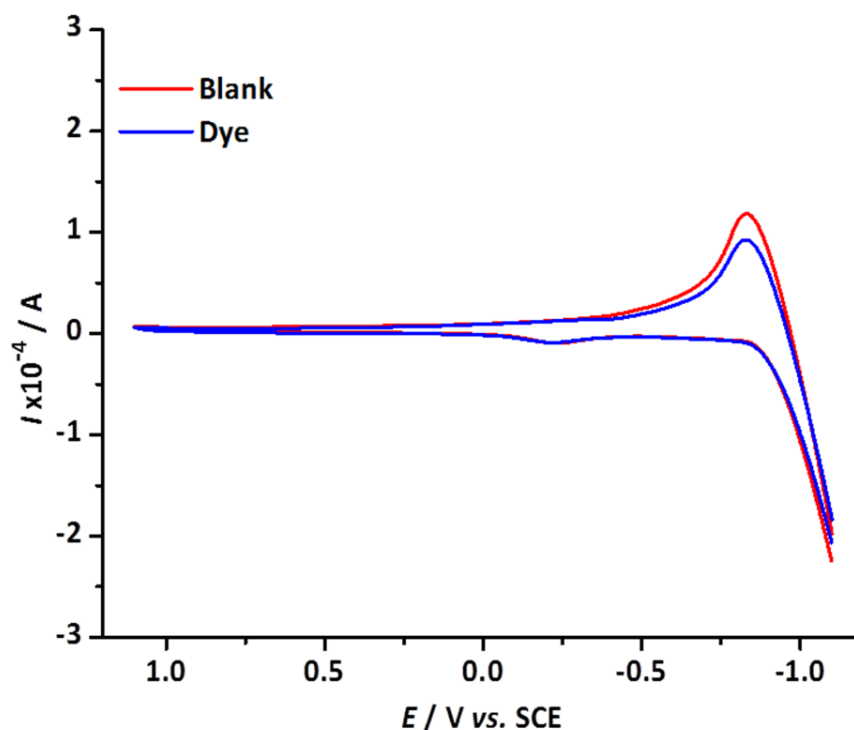
**Figure 1.** *CV of 0.2 % NaCl and 50 mg L$^{-1}$ TB + 0.2 % NaCl solutions; scan rate 100 mV s$^{-1}$*

*Effect of Supporting Electrolyte*

To determine the effect of different supporting electrolytes, preliminary investigations on TB degradation were carried out separately in presence of chloride ($Cl^-$), sulfate ($SO_4^{2-}$), nitrate ($NO_3^-$) and carbonate ($CO_3^{2-}$) ions. In all the cases 34.2 mM solution of electrolyte was was used. On electrolysis of the solution for 60 min, showed a 100 %, 42 %, 27 %, 15 % color removal in presence of $Cl^-$, $CO_3^{2-}$, $NO_3^-$, $SO_4^{2-}$ ions respectively. Similar trend was observed by Fornazari *et al.* [27] in the electrochemical degradation of phenol-formaldehyde mixture [27,28]. The presence of $Cl^-$ ions is not only essential for the color removal but also its *in situ* generated oxidants cleave the TB bonds. Therefore, NaCl was selected as the supporting electrolyte for the present studies. Fig. 2A and Fig. 2B depict the effect of different electrolytes on absorption intensity and color removal of dye.

The Pt is an active anode and during electrolysis the generation of hydroxyl radical is limited [6]. In presence of $CO_3^{2-}$, $NO_3^-$, $SO_4^{2-}$ ions, the oxidation of TB is possible only either by the hydroxyl radicals generated on Pt anode or by direct electron transfer with the anode. But Pt anode does not show any electrochemical activity for the oxidation of TB (Fig. 1). On Pt, in presence of oxygen and above 0.8 V there exists Pt and PtO mixture [29]. Slight decolorization of TB in presence $CO_3^{2-}$, $NO_3^-$, $SO_4^{2-}$ ions is perhaps due to oxidation by the hydroxyl radicals generated on Pt and by PtO/Pt couple. Below are the possible reactions (4) – (7) on the surface of the Pt anode [19,30].

$$Pt + H_2O \rightarrow Pt\text{-}OH_{ads} + H^+ + e^- \tag{4}$$

$$Pt\text{-}OH_{ads} \rightarrow PtO + H^+ + e^- \tag{5}$$

$$xPtO + R_{aq} \rightarrow ROx + xPt \tag{6}$$

$$2PtO \rightarrow 2Pt + O_2 \tag{7}$$

Decoloration is the clear evidence for the cleavage of the chromophoric (–N=N-) group of TB dye. Since decolorization was very slow in presence of $CO_3^{2-}$, $NO_3^-$, $SO_4^{2-}$ electrolytes, hence the COD removal cannot be more than color removal and is very small. Therefore COD was not measured in these cases.
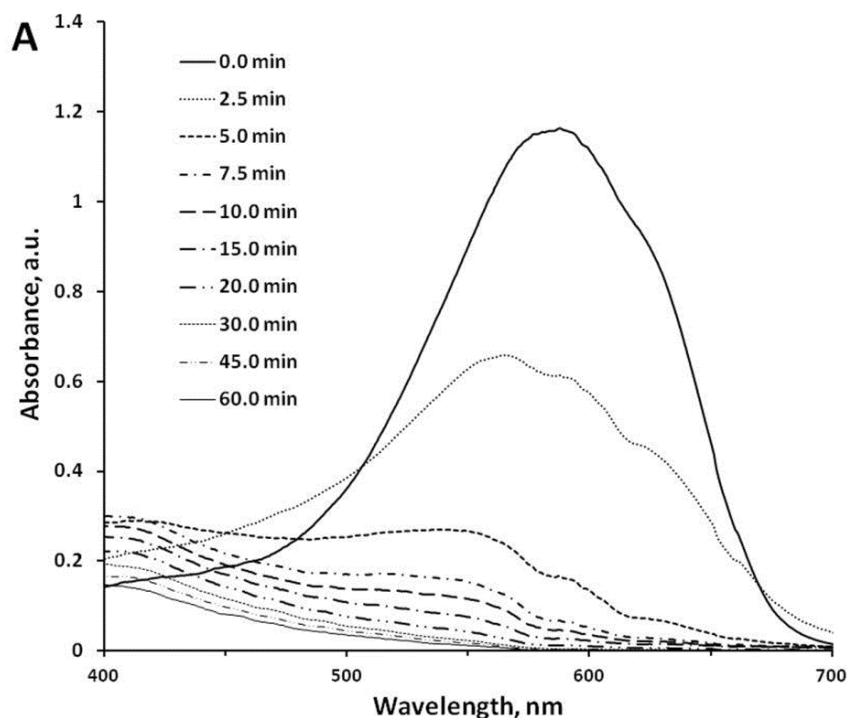


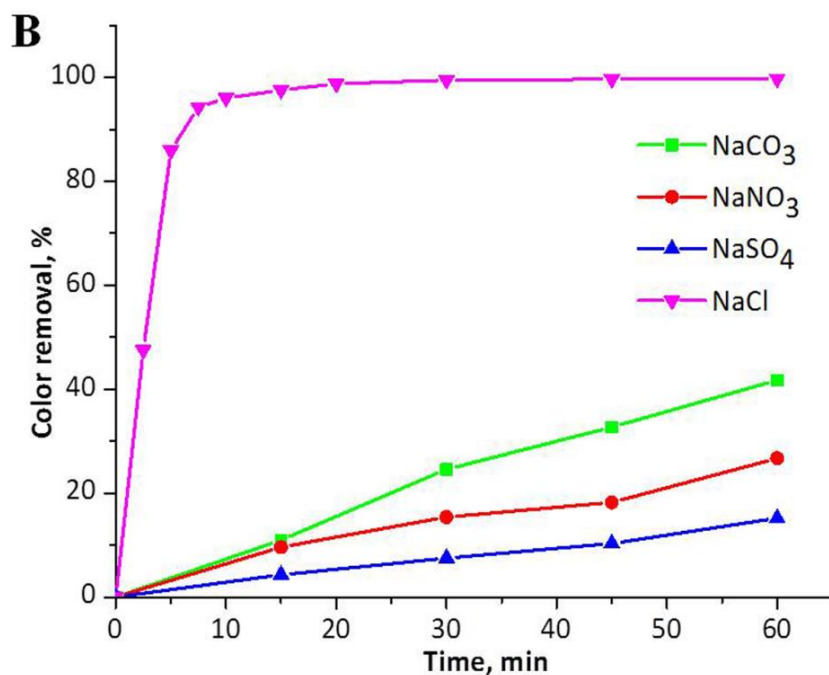**Figure 2A.** *The variation of absorption with electrolysis time. Conditions; 0.2% NaCl + 50 mg L$^{-1}$ TB, current density – 93 mA cm$^{-2}$, $\lambda_{max}$ = 590 nm*



**Figure 2B.** *Effect of supporting electrolytes on color removal*

Decoloration is the clear evidence for the cleavage of the chromophoric (–N=N-) group of TB dye. Since decolorization was very slow in presence of $CO_3^{2-}$, $NO_3^-$, $SO_4^{2-}$ electrolytes, hence the

COD removal cannot be more than color removal and is very small. Therefore COD was not measured in these cases.

*Effect of NaCl Concentration*

The effect of NaCl concentration on the rate of color and COD removal was investigated with NaCl concentration ranging from 0.05 % to 3.0 %. Fig. 3A and 3B, show the effect of NaCl on color and COD removal respectively.
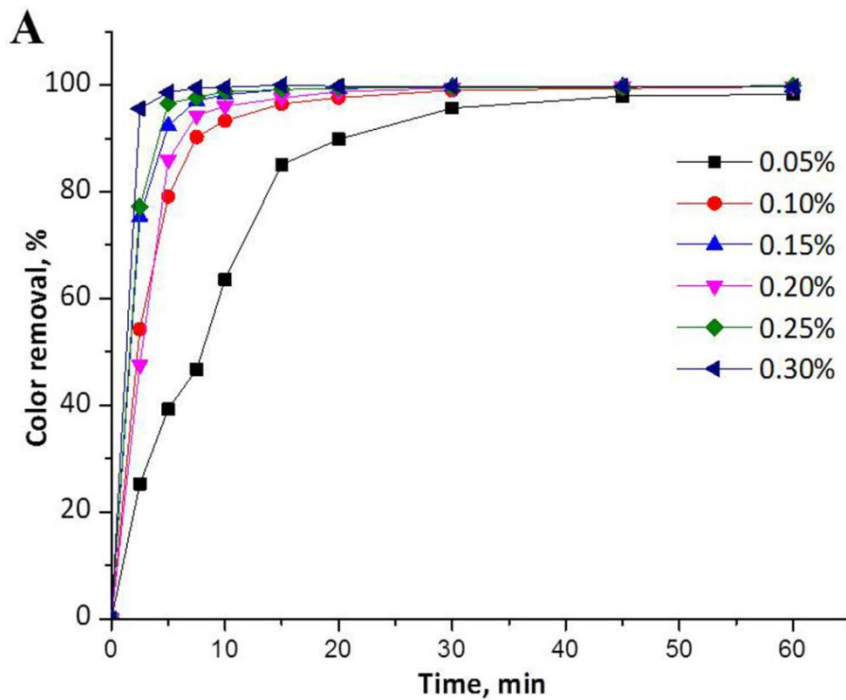


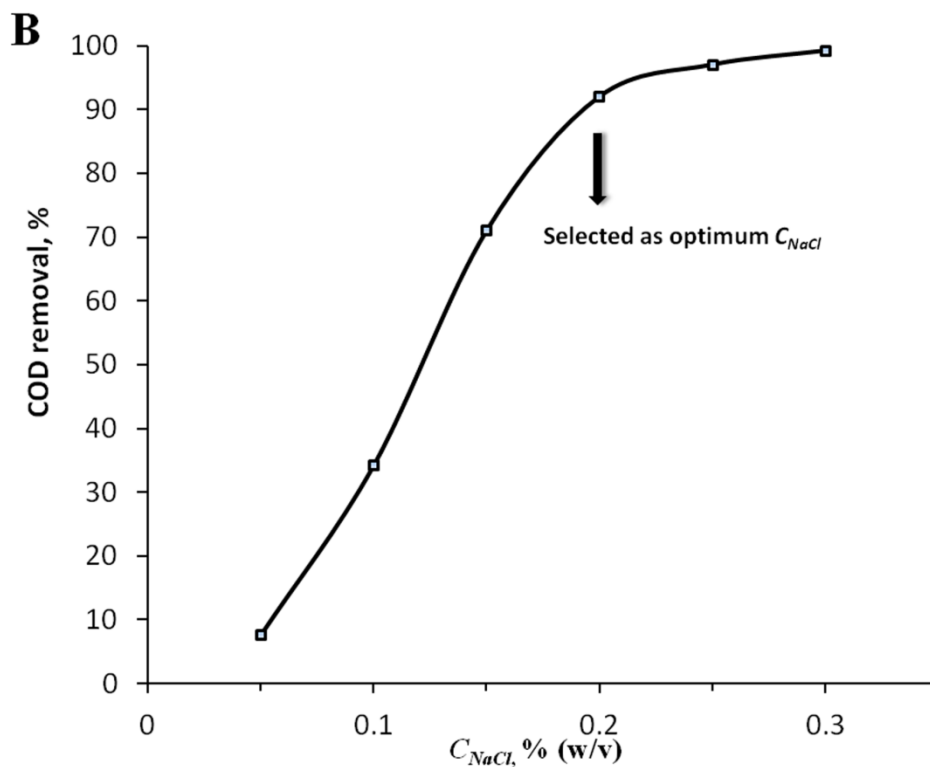***Figure 3A.** Effect of NaCl concentration on color removal*



***Figure 3B.** Effect of NaCl concentration on COD removal (electrolysis time 60 min)*

The amount of oxidants on the anode surface increases with the applied current density. But, at the given current density, the amount of Cl$^-$ ions is the limiting factor. If Cl$^-$ ion concentration in the solution is less, the current supplied would be lost in oxygen evolution, which is otherwise could be used to generate active chlorine species. The optimum Cl$^-$ ion concentration can facilitate high current efficiency and thus less energy consumption. At higher concentrations of Cl$^-$ ions, the applied current density is efficiently utilized to generate more oxidants [6]. At the same time, the concentration of Cl$^-$ ions should not exceed the concentration level commonly found in any real wastewater sample. So, the effect of Cl$^-$ ion concentration was tested within 0.3 % NaCl.

Complete decolorization of TB solution occurred in 30 min of electrolysis with all concentrations of NaCl from 0.1 % to 0.3 %, except with 0.05 % NaCl, in which 98 % color removal was achieved. The rate of decoloration increased with increase in Cl$^-$ ion concentration. Concomitant COD removal was observed with decolorization. The COD removal after 60 min electrolysis increased largely with NaCl concentration from 0.05 % to 0.2 %. After this concentration, only slight improvement in the COD removal was noticed. Therefore, 0.2 % NaCl was chosen as the optimum concentration for further studies.

*Effect of Current Density*

The efficiency and energy consumption for the degradation process is dependent on the applied current density and electrolysis time. Higher current density always leads to high energy consumption and low current efficiency. The degradation of TB in the present case takes place by indirect oxidation brought about by the oxidants generated during electrolysis. Higher current density enhances the rate of electrode reactions and hence rate of generation of oxidants also elevates. A range of current density from 37 to 111 mA cm$^{-2}$ was applied to determine its effect on color and COD removal. The rate of color and COD removal increased with applied current density (Fig. 4A and 4B). The COD removal increased as current density increased from 37 to 55 mA cm$^{-2}$, beyond which slow and steady raise in COD was noticed. In contrast, the current efficiency decreased with increse in applied current density.
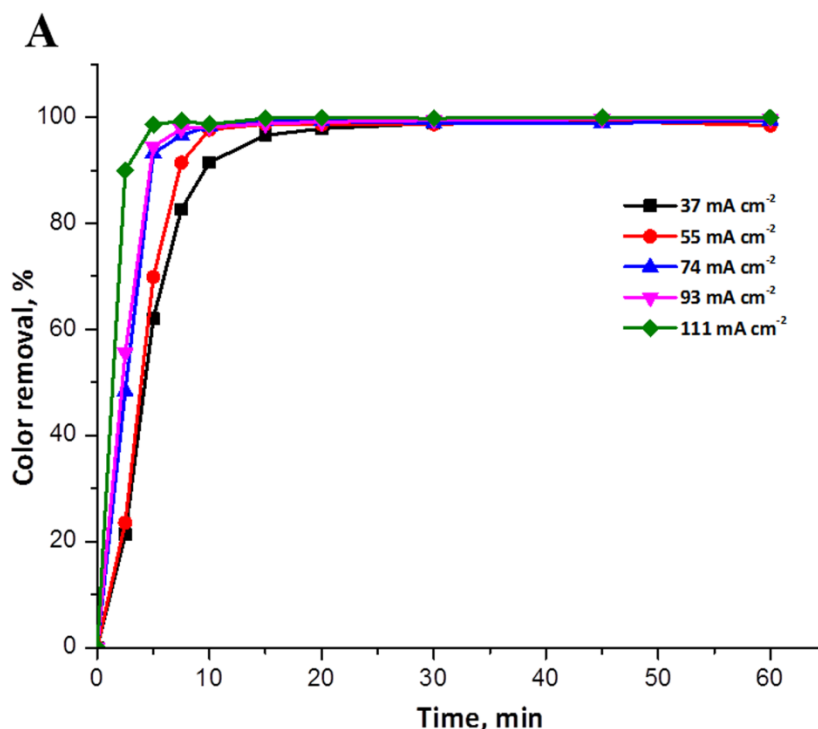


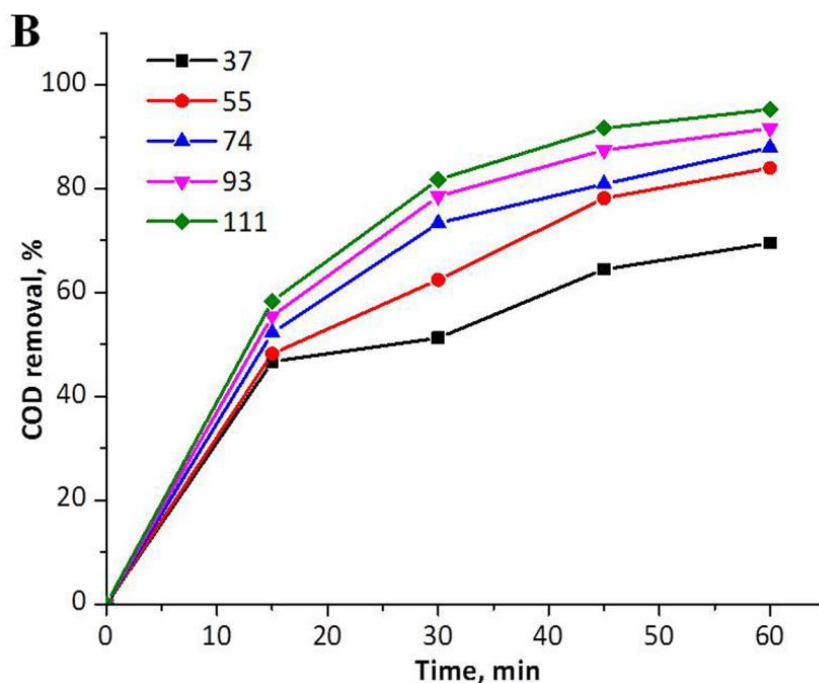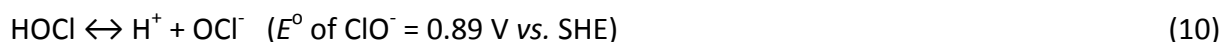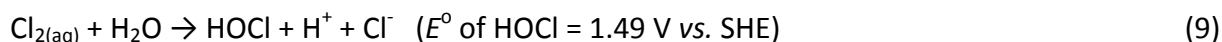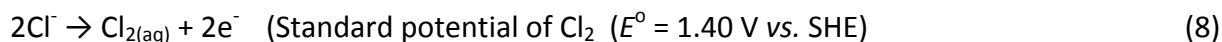**Figure 4A.** *Effect of current density on color removal*

**Figure 4B.** *Effect of current density on COD removal; conditions - 0.2 % NaCl, current density- 93 mA cm$^{-2}$, dye – 50 mg L$^{-1}$; electrolysis time – 60 min*

The color removal was 100 % in all cases and the COD removal was 70 % to 95 % with 25 % to 11 % current efficiency. This implies that with increase in current density, though the production of oxidants increased, the undesired hydrogen and oxygen evolution reactions also increased alongside and consumed major part of the supplied current. A charge consumption of 3.60 kC L$^{-1}$ was recorded for 92 % of COD removal under the current density of 93 mA cm$^{-2}$ (60 min) whereas, 2.88 kC L$^{-1}$ charge was consumed for the same COD removal under the current density of 37 mA cm$^{-2}$ (120 min). This indicates that higher COD removal can be achieved with less charge (and hence energy) consumption, but requires longer time duration.

*Effect of pH*

pH influences the chemical form of the oxidant present in the electrolyte. The electrolysis was carried out at four different pH. The electrochemical reaction in presence of chloride ions can be represented as in reactions (8) – (11);

$$2Cl^- \rightarrow Cl_{2(aq)} + 2e^- \quad \text{(Standard potential of } Cl_2 \; (E^o = 1.40 \text{ V } vs. \text{ SHE)} \qquad (8)$$

$$Cl_{2(aq)} + H_2O \rightarrow HOCl + H^+ + Cl^- \quad (E^o \text{ of } HOCl = 1.49 \text{ V } vs. \text{ SHE)} \qquad (9)$$

$$HOCl \leftrightarrow H^+ + OCl^- \quad (E^o \text{ of } ClO^- = 0.89 \text{ V } vs. \text{ SHE)} \qquad (10)$$

$$TB + OCl^- \rightarrow \text{Intermediates} \rightarrow CO_2 + H_2O + Cl^- \qquad (11)$$

The pH variation influences the equilibrium in reaction (10) and the HOCl predominates in the pH range 3-8 but above pH 8, ClO$^-$ is the major candidate [26,31]. The oxidation by HOCl and Cl$_{2(aq)}$ [5,6] is therefore expected to be more favorable and faster at near neutral pH. Furthermore, reactions in reaction (12) and (13) are expected to take place on the active anode such as Pt. The MOx(HOCl) mediates the oxidation unselectively and hence higher COD removal efficiency was noticed [26].

$$MOx(\bullet OH) + Cl^- \rightarrow MOx(HOCl) + e^- \tag{12}$$

$$MOx(HOCl) + TB \rightarrow Intermediates \rightarrow MOx + CO_2 + H_2O + Cl^- + H^+ \tag{13}$$

The effect of pH on color and COD removal with electrolysis time is shown in Figs. 5A and 5C, respectively. Fig. 5B illustrates the slow decrease in the absorption intensity of the peak in the visible region with increase in pH (11.8).  It is evident that color and COD removal is above 90 % in pH 3.1 and 6.2. As the pH increased to 9.0, the rate of color and COD removal reduced to 82 % and became 67 % in pH 11.8.
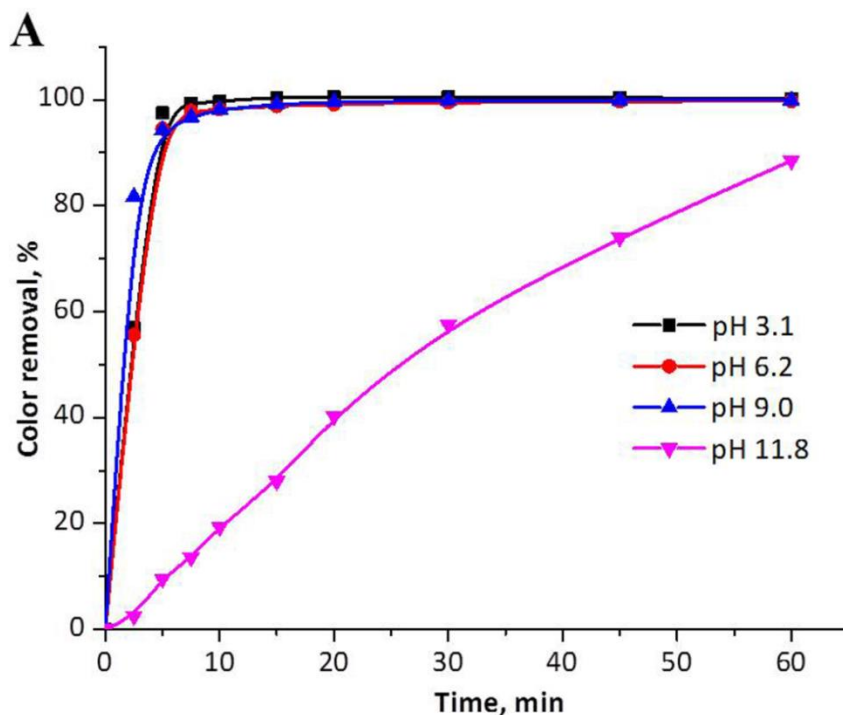


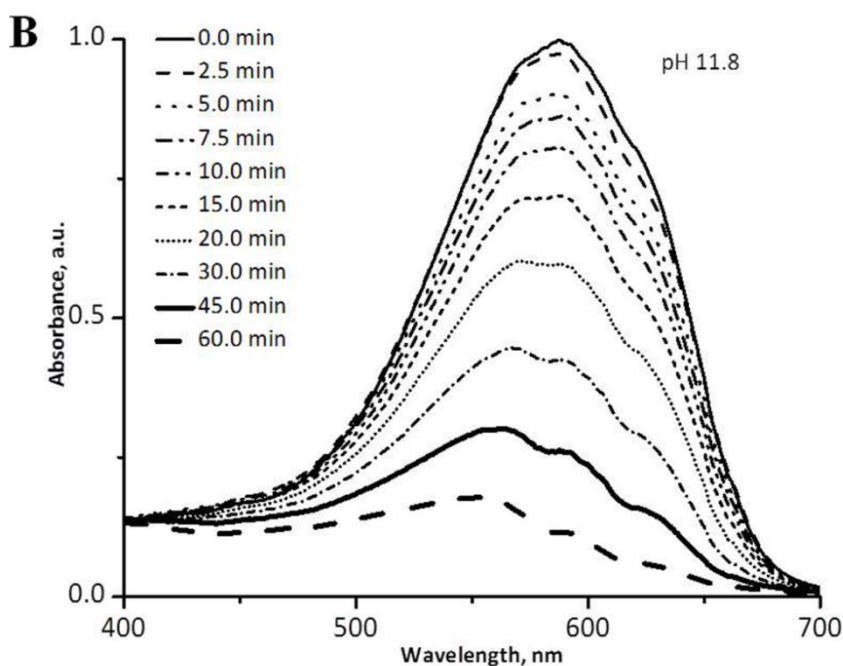**Figure 5A.** *Effect of pH on color removal*



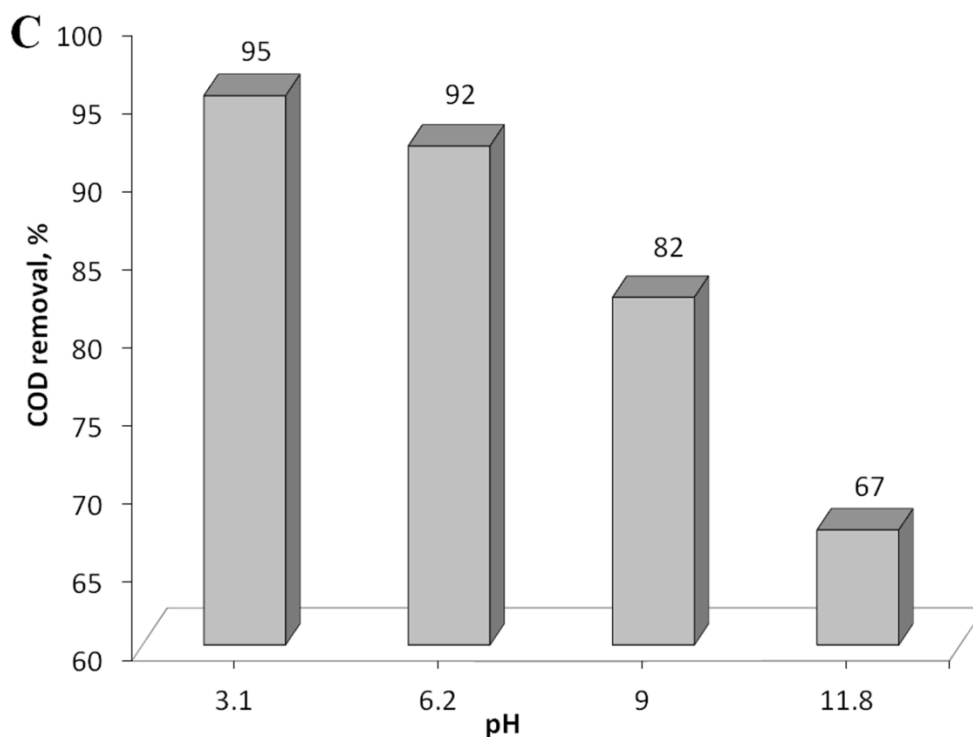**Figure 5B.** *Variation in the intensity of peak at 590 nm in pH 11.8*

**Figure 5C.** *Effect of pH on COD removal; conditions* $c_{NaCl}$, *0.2 % (w/v), current density – 93 mA cm$^{-2}$, [TB] – 50 mg L$^{-1}$, electrolysis time – 60 min*

Complete decoloration was achieved in all pH except with pH 11.8, for which 88 % color removal was achieved. The difference in COD removal in pH 3.1 and pH 6.2 was only 3 % and in both the cases it was above 90 %. But COD removal decreased above pH 9.0. Hence, for further studies, pH 6.2 was selected.

*Effect of Initial Dye Concentration*

At the optimized operating conditions of electrolysis process, only fixed amount of oxidants are generated at the anode. The energy would be simply lost if the generation of oxidants is more than that required to oxidize the available organics in the wastewater. Sufficient concentration of organics should be available for the efficient utilization of generated oxidants. The TB solutions of different concentrations ranging from 25 to 100 mg L$^{-1}$ were prepared and electrolysed under optimized operating conditions (93 mA cm$^{-2}$, pH 6.3 and 0.2 % NaCl concentration). The color and COD removal decreased gradually with increase in initial concentration of TB. Fig. 6 shows the trend of color and COD removal with time for different initial concentrations of TB dye. A 100 % decolorization was achieved within 30 min for all initial concentrations of TB. But 100, 91, 75 and 67 % COD removal was attained with 25, 50, 75 and 100 mg L$^{-1}$ initial TB concentrations respectively after 60 min electrolysis.

At initial concentration of 25 mg L$^{-1}$, the in situ generated oxidants were efficienty oxidized the TB completely. But, the dye concentration was less than the amount of oxidants available in the electrolysis cell (dye concentration is the limiting factor). When the TB dye concentration was increased to 100 mg L$^{-1}$, the amount of oxidants was less than the equivalent value, not sufficient to degrade the entire amount of TB (oxidant concentration is the limiting factor). Under the currrent density - 93 mA cm$^{-2}$ and 60 min of electrolysis, the COD removal was 92 % for the initial concentraiton of 50 mg L$^{-1}$ chosen as the optimum condition.
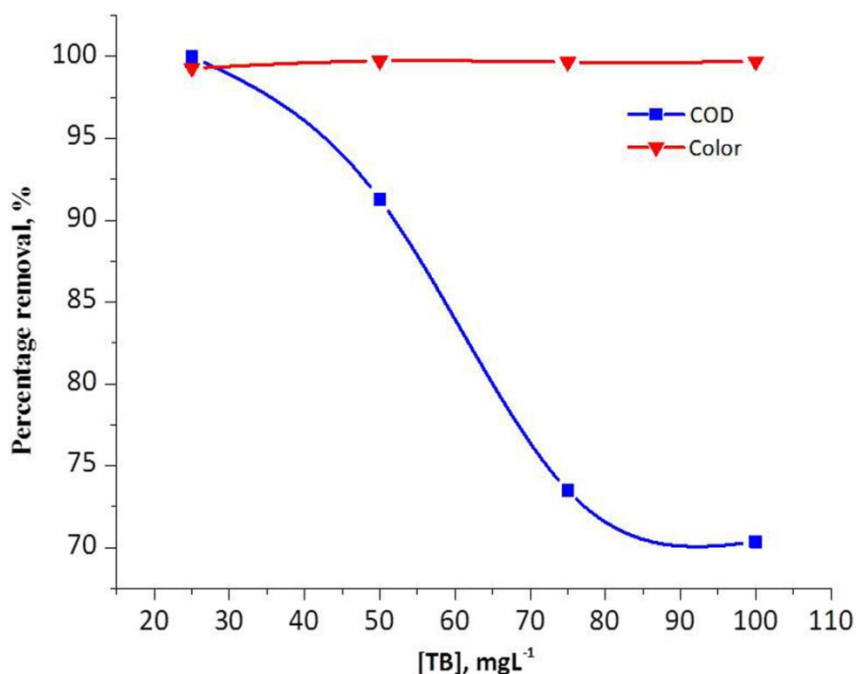
**Figure 6.** *Effect of initial concentration of TB on COD and color removal.*

### Kinetics of TB Degradation

During the electrolysis, the concentration of TB in synthetic wastewater decreased exponentially for all applied current densities but the rate of oxidation increased with increase in current density, indicating that the degradation of TB followed the first order kinetics [32]. If we consider that the oxidants generated on electrolysis spontaneously react with TB, then from the steady state approximation, the concentration of oxidants (Ox) can be estimated [32] and the rate of oxidation of TB can be expressed as in Eq. (13) and (14);

**Table 2.** *Degradation kinetics data*

| Parameters | $j$ / mA cm$^{-2}$* | | | | | Initial concentration of TB, mg L$^{-1}$# | | | |
|---|---|---|---|---|---|---|---|---|---|
|  | 37 | 55 | 74 | 93 | 111 | 25 | 50 | 75 | 100 |
| $k_{app}$ / min$^{-1}$ | 0.022 | 0.032 | 0.037 | 0.044 | 0.053 | 0.058 | 0.043 | 0.026 | 0.021 |
| Regression | 0.867 | 0.978 | 0.967 | 0.974 | 0.993 | 0.974 | 0.986 | 0.92 | 0.841 |

* TB concentration - 50 mgL$^{-1}$;   # Current density - 93 mA cm$^{-2}$

$$\frac{d[COD]}{dt} = -k \, [Ox][COD] \tag{13}$$

$$= -k_{app} \, [COD] \tag{14}$$

On integrating the above equation;

$$Ln \frac{[COD]_0}{[COD]_t} = k_{app} \, t \tag{15}$$

where [Ox] is the concentration of oxidants, $k_{app}$ is the apparent pseudo first-order rate constant ([Ox] is considered as very high), $COD_0$ and $COD_t$ are the COD at time 0 and $t$ minutes of electrolysis respectively.

The slope gives $k_{app}$ which are tabulated in Table II. The first order rate constant steadily increased with increase in applied current density and decreases with increase in initial

concentration of TB dye (Fig. 7A and 7B). The regression value indicates the deviation from the first order reaction rate equation for current density 37 mA cm$^{-2}$ and TB concentration 100 mg L$^{-1}$ can be attributed to the fact that at lower applied current density and high initial concentration of TB, the active concentration of oxidants is the limiting factor. Moreover, the area of the anode used in all these experiments was only 0.57 cm$^{2}$.
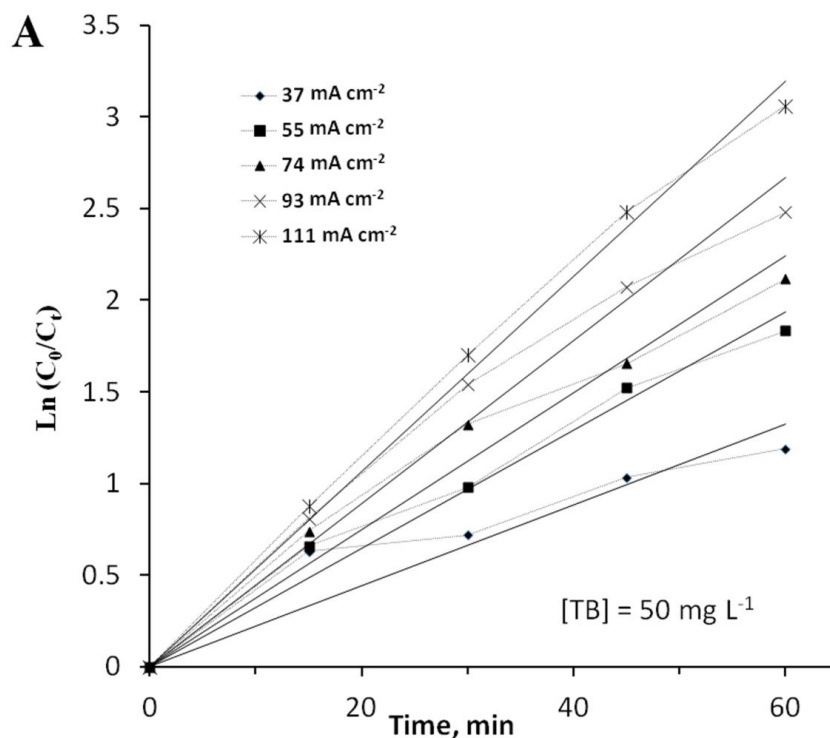


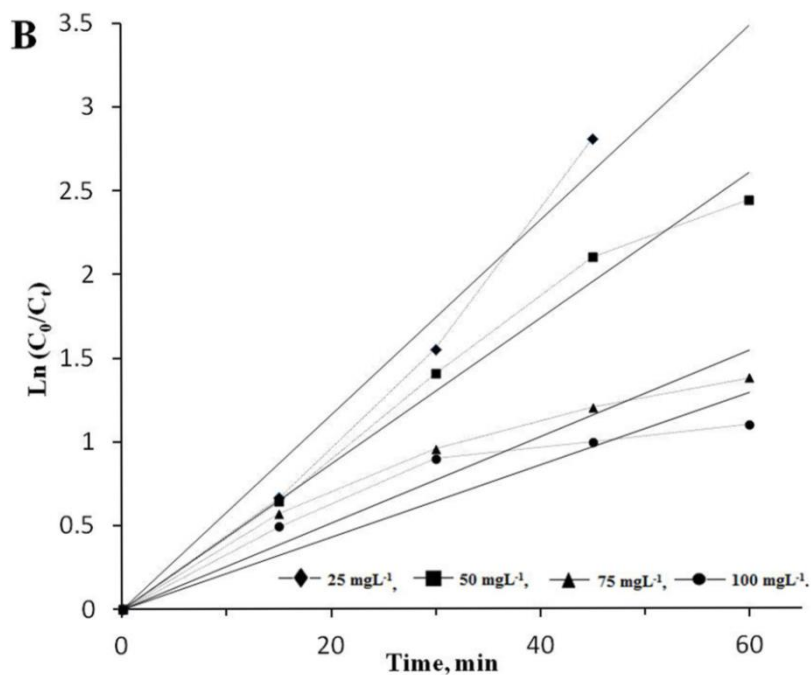**Figure 7A.** *Plot of ln (C$_0$/C$_t$) vs. time for different applied current densities*



**Figure 7B.** *Plot of ln(C$_0$/C$_t$) vs time for different initial dye concentrations*

The oxidants generated on the surface of such a small area of Pt anode under the current density of 37 mA cm$^{-2}$ might not be so high to satisfy the steady state approximation for first order

kinetics. Similarly, oxidants generated under the current density of 93 mA cm$^{-2}$ and 100 mg L$^{-1}$ initial concentration of TB dye, a similar deviation was observed.

*Spectroscopic Analysis*

UV-vis spectroscopic analysis

UV-Vis spectrum of TB dye showed three major peaks at 235, 318 and 590 nm. The peak at 590 nm corresponds to the chromophoric azo group. On electrolysis (50 mgL$^{-1}$ dye, 93 mAcm$^{-2}$), the intense blue color of the solution turned in to wine red in the first 10 min, then transformed slowly into pale yellow color, which persisted till the end. The intensity of the peak at 590 nm rapidly decreased to zero absorbance on electrolysis, which can be ascribed to the cleavage of azo group.
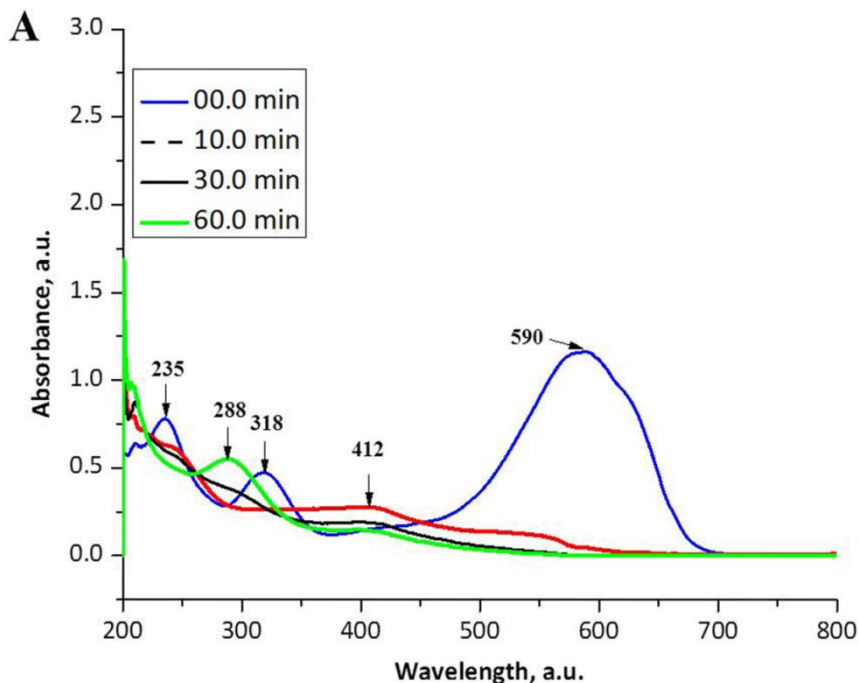


***Figure 8A.*** *UV-Visible absorbance of TB at different time intervals of electrolysis*
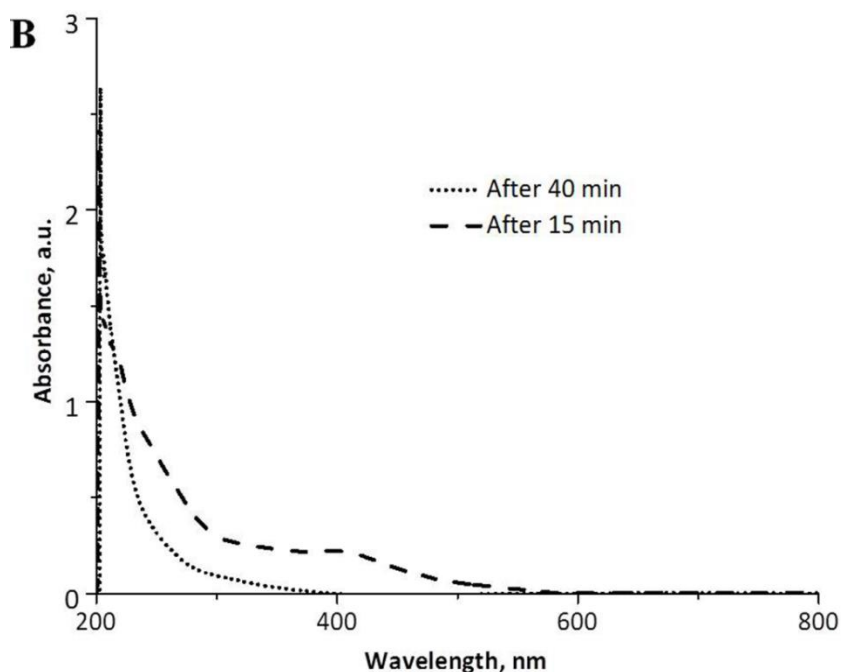


***Figure 8B.*** *Absorbance of residue obtained by the evaporation of electrolyzed TB solution*

For the first 10 min of electrolysis, the peak at 585 nm showed blue shift and gradually reached zero absorbance. The blue shift can be attributed to the detachment of auxochromes from the parent dye structure during electrolysis. A new peak at 407 nm was observed, which can be ascribed to the formation of a fragment from the parent dye. This peak diminishes very slowly. The pale yellow color is due to the absorption at 412 nm, (absorption color – violet (412 nm), perceived color – yellow) which reduced slowly with time (Fig. 8A). Peak at 318 nm reduced with time, reached minimum value and again increased with a blue shift at 288 nm. This peak can be assigned to the low molecular weight oxidized fragments with conjugated π bonds in which n→π* and π→π* transitions are allowed (-C=O, -C=C-, -C=N-, -(CO)NH-). Similar effect was observed by Hanene et al. [34] in the degradation of Amido black (AB) on boron doped diamond electrode.

The electrolyzed dye solution was evaporated at lower temperature with reduced pressure. UV-Vis spectrum of the solid thus obtained was taken by dissolving it in water. Interestingly, the peak at 288 nm was absent. This observation validates our suspicion that compounds leading to this peak were low molecular volatile compounds (Fig. 8B). After 40 min electrolysis, the UV-Vis spectrum of the residue obtained by evaporation does not show any peak, except a peak in 200 to 220 nm range. This is due to the small amount of aromatic compounds resistant to indirect oxidation remained in the solution, which also accounts for the residual COD after 60 min.

FT-IR analysis

The FT-IR spectrum of TB dye (Fig. 9A) exhibits a characteristic band at 1579 cm$^{-1}$ corresponding to azo group [34, 35]. The bands at 1492 cm$^{-1}$ and 1423 cm$^{-1}$ correspond to C=C aromatic ring stretching in combination with C=N [34] and methyl bending respectively. The keto form of the TB is dominant (Table I) [36]. The peak at 1617 cm$^{-1}$ is due to α,β-unsaturated C=O stretch. The peaks at 1339, 1188 and 1128 cm$^{-1}$ are due to aromatic amine C-N and -SO$_3^-$ (S=O) stretch [35]. The peak obtained at 1042 cm$^{-1}$ is due to C-O. The broad doublet peak at 674 cm$^{-1}$ and 644 cm$^{-1}$ indicates the aromaticity. In Fig. 9B and 9C, the peaks at 1579, 1492, 1423 cm$^{-1}$ and 1339, 1128, 1042, 674 cm$^{-1}$ disappeared completely indicating the breakage of corresponding groups.
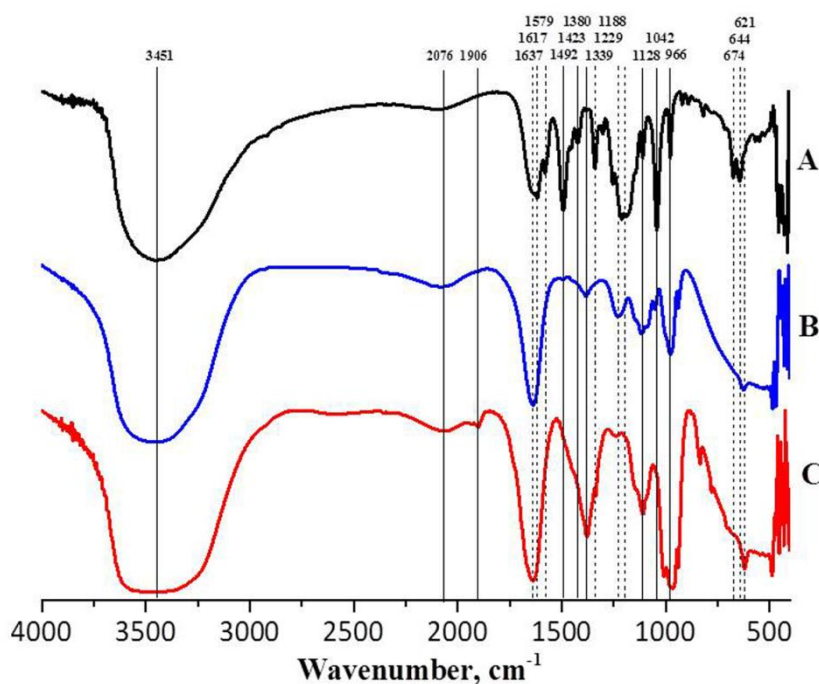


**Figure 9.** *FT-IR spectra of A) TB dye B) residue obtained by evaporation of sample electrolyzed for 15 min C) electrolyzed for 40 min*

The peak at 1229 cm$^{-1}$ disappeared in Fig. 9C, indicating that group corresponding to this frequency is susceptible to oxidation by the electrochemically generated oxidants [37]. The peak at 1119 cm$^{-1}$ shifted to 1108 cm$^{-1}$. While peak 674 cm$^{-1}$ disappeared completely, 644 cm$^{-1}$ shifted to 621 cm$^{-1}$. In Fig. 9C the peak at 1637 cm$^{-1}$ is due to the carbonyl stretch of carboxylate salts, 1380 cm$^{-1}$ is due to C-N of aliphatic amines. This suggests the formation of carboxylic acids and amines. 1008 cm$^{-1}$ is devoted to C-O stretch and peak at 966 cm$^{-1}$ is due to the formation of $ClO_3^-$ and $OCl^-$ during electrolysis [34,35]. These changes in the FT-IR spectrum are the clear evidence for the degradation of TB into simpler molecules, like aromatic and aliphatic amines and carboxylic acids.

Identification of intermediate products and degradation pathway

The intermediates of TB degradation were identified by gas chromatography mass spectrometry (GC-MS). On the basis of the intermediates and end products as depicted by GC-MS, a possible degradation pathway is proposed in Fig. 10. GC-MS revealed that the parent TB molecule was completely disintegrated into simpler molecules.
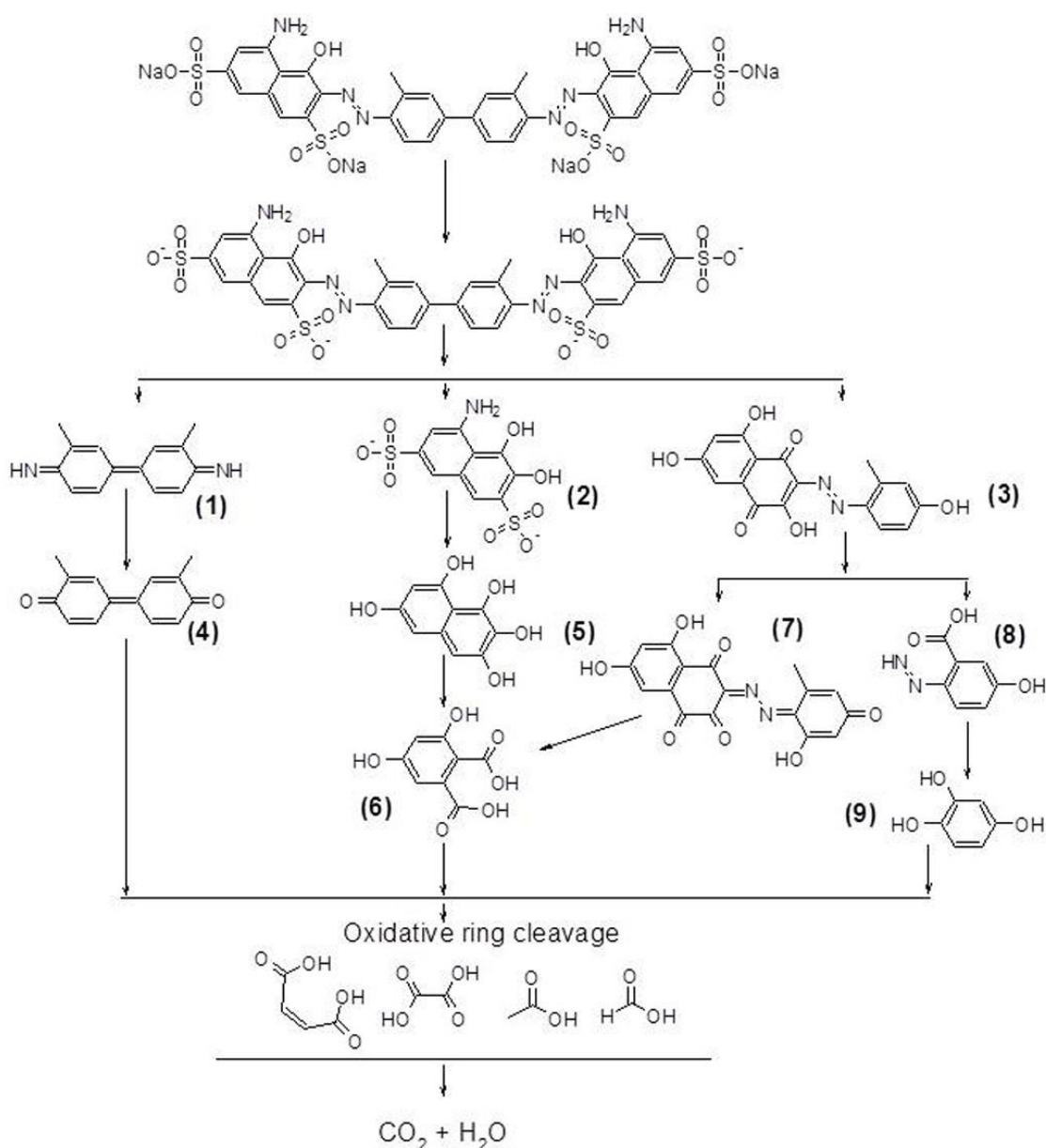


**Figure 10.** *A possible degradation pathway of TB*

Decomposition of TB was initiated with the cleavage of azo bonds resulting in the formation of three different intermediates **1** (3,3'-dimethyl-1,1'-bi(cyclohexa-2,5-dien-1-ylidene)-4,4'-diimine), **2** (5-amino-3,4-dihydroxynaphthalene-2,7-disulfonic acid) and **3** (2,5,7-trihydroxy-3-[(4-hydroxy-2-methylphenyl)diazenyl]naphthalene-1,4-dione). Intermediate **3** resulted from the cleavage of one of the azo bonds in the parent molecule was found in very small concentration. The absorption at 412 nm in UV-Vis spectroscopy can be attributed to this intermediate. The sulfonic group in intermediate **2** renders it water soluble. A foamy layer was formed on the surface of the electrolytic bath solution during electrolysis gradually disappeared with time. This can be attributed to the formation of intermediates **1** and **3** at the beginning of electrolysis. Further oxidation of intermediates **2** and **3** produced aromatic acids and phenols, **5** (naphthalene-1,2,3,6,8-pentol), **6** (3,5-dihydroxybenzene-1,2-dicarboxylic acid), **9** (benzene-1,2,4-triol). Aliphatic acids were generated on the oxidative ring opening of **4**, **6** and **9**, which decomposed into $CO_2$ to accomplish the degradation process.

## Conclusion

The TB dye synthetic wastewater was successfully treated in presence of $Cl^-$ with Pt foil as anode material. The removal of TB was dependent on the applied current density, pH, type of supporting electrolyte and concentration of TB dye and NaCl. The degradation of TB was achieved only in presence of NaCl as supporting electrolyte suggesting that the active chlorine species ($Cl_2$, $ClO^-$, HOCl) generated during the electrolysis played crucial role in the oxidation of TB. The rate of removal of TB increased with increase in current density and NaCl concentration and decreased with rise in initial concentration of TB and pH. Under the optimum conditions (current density – 93 mA cm$^{-2}$, pH - 6.2, NaCl concentration - 0.2 %, initial TB concentration – 50 mgL$^{-1}$) maximum COD and color removal achieved after 60 min electrolysis was 92 % and 100 % respectively. The first order rate constant for COD removal at these conditions was 0.044 min$^{-1}$. The UV-Vis spectroscopy, FT-IR and GC-MS analysis confirmed the complete degradation of TB into simple aliphatic carboxylic acid and $CO_2$ suggesting that the treatment of wastewater containing TB dye as pollutant can be successfully accomplished by electrochemical method.

## References

[1]   H. Zollinger, Synthesis, Properties of Organic Dyes and Pigments. In: Color Chemistry. New York, USA: VCH Publishers; (1987) pp-92-102

[2]   M. B. Ibrahim, N. Poonam, S. Datel, M. Roger, *Bioresour Technol.* **58** (1996) 217-227

[3]   E. Forgacs, T. Cserháti, G. Oros, *Environ Inter.* **30** (2004) 953971

[4]   W. Przystaś, E. Zabłocka-Godlewska, E. Grabińska-Sota, *Water, Air, Soil Pollut.* **223** (2012) 1581-1592

[5]   S. Song, J. Fan, Z. He, L. Zhan, Z. Liu, J. Chen, X. Xu, *Electrochim. Acta* **55** (2010) 3606-3613

[6]   C. A. Martinez-Huitle, E. Brillas, *Appl Catal B: Environ* **87** (2009) 105-145

[7]   F. Zaviska, P. Drogui, J. F. Blais, G. Mercier, *J. Appl. Electrochem.* **39** (2009) 2397-2408

[8]   J. L. Nava, M. A. Quiroz, C. A. Martínez-Huitle, *J. Mex. Chem. Soc.* **52** (2008) 249-255

[9]   E. Kusmierek, E. Chrzescijanska, M. Szadkowska-Nicze, J. Kaluzna-Czaplinska, *J. Appl. Electrochem.* **41** (2011) 51–62.

[10]  R. G. da Silva, S. A. Neto, A. R. de Andrade, *J. Braz. Chem. Soc.* **22** (2011) 126-133

[11]   T. Panakoulias, P. Kalatzis, D. Kalderis, A. Katsaounis, *J. Appl. Electrochem.* **40** (2010) 1759-1765

[12]   L. Jiancheng, Y. Jie, L. Weishan, H. Qiming, X. Hongkang, *J. Electrochem. Sci. Eng.* **2** (2012) 171-183

[13]   D. A. Carvalho, J. H. B. Rocha, N. S. Fernandes, D. S.  da Silva, C. A. Martínez-Huitle, *Latin Am. Appl. Res.* **41** (2011) 127-133

[14]   M. Panizza, G. Cerisola, *Ind. Eng. Chem. Res*. **47** (2008) 6816-6820

[15]   J. Marugán, M. J. López-Muñoz, R. van Grieken, J. Aguado, *Ind. Eng. Chem. Res.* **46** (2007) 7605-7610

[16]   Health Hazard Alert - Benzidine-, o-Tolidine-, and o-Dianisidine- Based Dyes. NIOSH Report DHEW (NIOSH) Publication No. 81-106, December 1980.

[17]   H. B. Mansour, D. Corroler, D. Barillier, K. Ghedira, L. Chekir, R. Mosrati, *Food Chem. Toxicol.* **45** (2007) 1670-1677

[18]   Toxicology data network, National Library of Medicine, Hazardous Substance Data Bank (HSDB), U.S department of Health and Human services. http://toxnet.nlm.nih.gov/cgi-bin/sis/search/f?./temp/~s8y7RI:1, August, 2013

[19]   P. Jiang, J. Zhou, A. Zhang, Y. Zhong, *J. Environ. Sci.* **4** (2010) 500-506

[20]   V. Jhanji, E. Chan, S. Das, H. Zhang, R. B. Vajpayee, *Eye* **25** (2011) 1113-1120

[21]   C. Lüke, M. Lüke, T. S. Dietlein, A. Hueber, J. Jordan, W. Sickel, B. Kirchhof, *Br. J. Ophthalmol.* **89** (2005) 1188-1191

[22]   B. T. van Dooren, W. H. Beekhuis, E. Pels, *Arch. Ophthalmol.* **122** (2004) 736-742

[23]   M. Veckeneer, K. van Overdam, J. Monzer, K. Kobuch, W. van Marle, H. Spekreijse, J. van Meurs, *Graefe's Arch. Clin. Exp. Ophthalmol.* **239** (2001) 698-704

[24]   M. M. Turbow, *Nature,* **206** (1965) 637.

[25]   C. H. Waddington, M. M. Perry, *J. Embryol. Exp. Morph.* **4** (1956) 110-119

[26]   S. A. Elfeky, A. S. A. Al-Sherbini, *Kinet and Catal.* **52** (2011) 391-396

[27]   A. L. T. Fornazari, G. R. P. Malpass, D. W. Miwa, A. J. Motheo, *Water, Air, Soil Pollut.* **223** (2012) 4895-4904

[28]   M. Gaber, N. A. Ghalwa, A. M. Khedr, M. F. Salem, *J. Chem.* **2013** (2013) 1-9

[29]   C. Song, J. Zhang, PEM fuel cell electrocatalysts and catalyst layers, fundamentals and applications, Spinger-Verlag London Limited, Vancouver, Canada, 2008, p. 89-134 http://www.springer.com/978-1-84800-935-6

[30]   R. B. Moghaddam, P. G. Pickup, *Electrochim. Acta* **97** (2013) 326-332

[31]   G. R. P. Malpass, D. W. Miwa, R. L. Santos, E. M. Vieira, A. J. Motheo, *Environ. Chem. Lett.* **10** (2012) 177-182

[32]   M. Panizza, G. Cerisola, *Chemosphere* **77** (2009) 1060-1064

[33]   H. Akrout, L. Bousselmi, *Arab. J. Geosci.* (2012) 5033-5041

[34]   H. Z. Zhao, Y. Sun, L. N. Xu, J. R. Ni, *Chemosphere* **78** (2010) 46-*51*

[35]   S. Raghu, C. W. Lee, S. Chellammal, S. Palanichamy, C. A. Basha, *J. Hazard. Mater.* **171** (2009) 748-754

[36]   J. P. Graham, M. A. Rauf, S.Hisaindee, M. Nawaz, *J. Molecul. Struc.* **1040** (2013) 1-8

[37]   S. S. Vaghela, A. D. Jethva, B. B. Mehta, S. P. Dave, S. Adimurthy, G. Ramachandraiah, *Environ. Sci. Technol,* **39** (2005) 2848-2855